Evidence for unnatural-parity contributions to electron-impact ionization of laser-aligned atoms

G. S. J. Armstrong,[1,2] J. Colgan,[2] M. S. Pindzola,[3] S. Amami,[4] D. H. Madison,[4] J. Pursehouse,[5]
K. L. Nixon,[6] and A. J. Murray[5]

[1]*J. R. Macdonald Laboratory, Department of Physics, Kansas State University, Manhattan, Kansas 66506, USA*
[2]*Theoretical Division, Los Alamos National Laboratory, New Mexico 87545, USA*
[3]*Department of Physics, Auburn University, Auburn, Alabama 36849, USA*
[4]*Physics Department, Missouri University of Science and Technology, Rolla, Missouri 65409, USA*
[5]*Photon Science Institute, School of Physics and Astronomy, University of Manchester, Manchester, M13 9PL England, United Kingdom*
[6]*Departamento de Fisica, UFJF, Juiz de Fora, MG 36036-330 Brazil*
(Received 27 June 2015; published 11 September 2015)

Recent measurements have examined the electron-impact ionization of excited-state laser-aligned Mg atoms. In this work we show that the ionization cross section arising from the geometry where the aligned atom is perpendicular to the scattering plane directly probes the unnatural parity contributions to the ionization amplitude. The contributions from natural parity partial waves cancel exactly in this geometry. Our calculations resolve the discrepancy between the nonzero measured cross sections in this plane and the zero cross section predicted by distorted-wave approaches. We demonstrate that this is a general feature of ionization from *p*-state targets by additional studies of ionization from excited Ca and Na atoms.

I. INTRODUCTION

The study of electron-impact single ionization of atomic and molecular targets [often known as (*e*,2*e*) studies] has long been a fruitful area of research in atomic collision physics, since it probes the delicate interactions between two outgoing electrons moving in a Coulomb field, i.e., electron-electron correlations [1]. Many fundamental experimental and theoretical studies have been reported for ionization of the simplest atomic systems, H [2–7] and He [8–13], and more recently for the simplest molecular system, H_2 [14–16].

Ionization from *excited* states of atoms has received much less attention due to the difficulty in preparing such targets. Significant advances in such studies were recently reported in experiments where a laser was used to excite Mg atoms into their $3s3p\,^1P$ state, which then were ionized by an incoming electron beam [17,18]. Moreover, the laser was used to prepare different alignment angles of the initial *p* orbital, allowing a probe of the angular distribution dependence on the orientation of the atomic orbital. Recent studies have also examined the angular distribution dependence of ionization of aligned molecular targets [19]. The experimental studies on Mg [17,18] were very recently compared to three-body distorted-wave (3DW) calculations [20], and reasonable agreement was found between most of the measured triple differential cross sections and the calculations. However, one striking difference was noted for cross sections measured when the aligned atom was perpendicular to the scattering plane (i.e., the *p* orbital was aligned along the *y* direction, see Fig. 1); the 3DW calculation predicted an identically zero cross section in this plane, at odds with the measurement that was clearly nonzero. The analysis of this zero cross section was also found to be consistent with other recent theoretical work [21].

In this paper we report close-coupling calculations for the triple differential cross sections from excited Mg atoms, and find that the cross section in the perpendicular geometry arises from the unnatural parity contribution to the ionization amplitude. An unnatural parity state is a state with parity $(-1)^{L+1}$ compared to a natural parity state that has parity $(-1)^L$. Our cross sections in this plane calculated using

a time-dependent close-coupling (TDCC) approach are in reasonable agreement with the measured data. We also show that similar nonzero cross sections should be observed in the perpendicular (*y*) geometry for any atomic *p* orbital and illustrate this with calculations of the triple differential cross sections from excited-state Na and Ca. For Ca, our calculations are in good agreement with new measurements of these cross sections, which are presented here.

II. THEORY

The TDCC theory as applied to electron-impact ionization has been well described [22,23]. The extension of the method to treat multielectron systems, by utilizing an orthogonalization to the filled subshells at each time step, was presented recently for calculations for the single ionization of ground-state Mg [24]. The calculations presented here follow this procedure, except that the active electron is now the $3p$ orbital of Mg. The Mg^+ [Ne]$3s$ core is the same as used in our previous calculations from the ground state [24]. We note that this approach is effectively a configuration-average approach to electron-impact ionization, that is, we consider only the $3p$ active orbital as a configuration and do not account for the term splitting of the $3s3p$ Mg configuration into the ^1P and ^3P terms. This differs somewhat from the measurement [17], since the laser excitation from the ground state in the experiment populates only the $3s3p\,^1P$ term. It is possible to use a three-electron TDCC approach (in which two bound electrons are active) to create an initial $3s3p\,^1P$ term and perform calculations of the single ionization of this term. Such calculations are, however, extremely computationally intensive and in this paper we discuss only test calculations made using this approach.

The two-electron TDCC approach centers around the solution of the set of partial differential equations given by

$$i\frac{\partial}{\partial t}P^{LS}_{l_1 l_2}(r_1,r_2,t) = [T_{l_1}(r_1) + T_{l_2}(r_2)]P^{LS}_{l_1 l_2}(r_1,r_2,t)$$
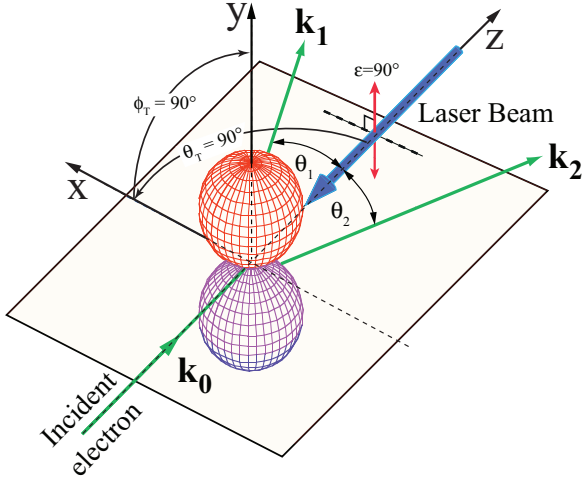$$+ \sum_{l'_1 l'_2} V^L_{l_1 l_2, l'_1 l'_2}(r_1,r_2) P^{LS}_{l'_1 l'_2}(r_1,r_2,t). \quad (1)$$

FIG. 1. (Color online) Geometry of the scattering experiments performed on Mg [17] and for the Ca experiments reported here. The incident electron has momentum $\mathbf{k}_0$ and the outgoing electrons have momentum vectors $\mathbf{k}_1$ and $\mathbf{k}_2$. The target p orbital is shown here to be aligned along the y axis using the laser beam polarization, i.e., perpendicular to the scattering plane (in which the outgoing electrons lie).

These equations are the result of the expansion of the total wave function over coupled spherical harmonics, and insertion of this expansion into the time-dependent Schrödinger equation. In Eq. (1) $T_l(r)$ represents the one-electron kinetic- and potential-energy terms, which include direct and local exchange potentials that describe the interaction with the inert core electrons, and $V(r_1, r_2)$ represents the electron-electron interaction potential. The initial $t = 0$ boundary condition is given by

$$P_{l_1 l_2}^{LS}(r_1, r_2, t = 0) = \frac{1}{\sqrt{2}} \big[P_{nl_1}(r_1) G_{k_2 l_2}(r_2) + (-1)^S G_{k_1 l_1}(r_1) P_{nl_2}(r_2) \big], \quad (2)$$

where in the present case $nl \equiv 3p$ and $G_{kl}(r)$ represents the incoming wave packet [22]. To compare against the measurements of [17,18], we must also take into account the orientation of the initial $3p$ orbital. We may do this by using a boundary condition of the form [25]

$$P_{l_1 l_2}^{LS}(r_1, r_2, t = 0) = \frac{1}{\sqrt{2}} \big[P_{nl_1}(r_1) \mathcal{R}_M G_{k_2 l_2}(r_2) + (-1)^S G_{k_1 l_1}(r_1) P_{nl_2}(r_2) \mathcal{R}_M \big], \quad (3)$$

where

$$\mathcal{R}_M = \Big[-\frac{1}{\sqrt{2}} e^{-i\phi_T} \sin\theta_T \delta_{M,-1} + \cos\theta_T \delta_{M,0} + \frac{1}{\sqrt{2}} e^{i\phi_T} \sin\theta_T \delta_{M,+1} \Big], \quad (4)$$

and the angles θ_T, ϕ_T define a given orientation of the initial p orbital with respect to the z axis, with the z axis defined along the incident electron-beam direction (see Fig. 1). Here M is the azimuthal quantum number of the oriented atom, since the wave packet has $m = 0$ by definition. Since the $\mathcal{R}_M$ term does

not depend on the coupled channels $l_1 l_2$, and since the TDCC Hamiltonian is independent of M, the time propagation of the coupled differential equations is unchanged by the $\mathcal{R}_M$ term in the initial boundary condition. This term will only affect the calculation of the triple differential cross sections, which take the form

$$\frac{d^3\sigma}{dE_1 d\Omega_1 d\Omega_2} = \frac{w_t}{(2l_t + 1)} \frac{\pi}{4k_0^2} \frac{1}{k_1 k_2} \sum_S (2S + 1) \int_0^\infty dk_1$$
$$\times \int_0^\infty dk_2 \, \delta\Big(\alpha - \tan^{-1}\frac{k_2}{k_1}\Big) |\mathcal{M}|^2, \quad (5)$$

where now

$$\mathcal{M} = \sum_L i^L \sum_{M=0,-1,+1} \Big[-\frac{1}{\sqrt{2}} e^{-i\phi_T} \sin\theta_T \delta_{M,-1} + \cos\theta_T \delta_{M,0}$$
$$+ \frac{1}{\sqrt{2}} e^{i\phi_T} \sin\theta_T \delta_{M,+1} \Big]$$
$$\times \sum_{l_1 l_2} (-i)^{l_1+l_2} e^{i(\sigma_{l_1}+\sigma_{l_2})} e^{i(\delta_{l_1}+\delta_{l_2})}$$
$$\times P_{l_1 l_2}^{LS}(k_1, k_2, T) \sum_{m_1 m_2} C_{m_1 m_2 M}^{l_1 l_2 L} Y_{l_1 m_1}(\theta_1, \phi_1) Y_{l_2 m_2}(\theta_2, \phi_2). \quad (6)$$

Note that the M dependence enters into both the first term and the coupled spherical harmonic in the last line of Eq. (6). In Eq. (5) w_t and l_t are the occupation number and angular momentum of the initial target orbital, and α is the angle in the hyperspherical plane between the two outgoing momentum vectors $\mathbf{k}_1$ and $\mathbf{k}_2$. In Eq. (6) $Y_{lm}(\theta, \phi)$ is a spherical harmonic, $C_{m_1 m_2 m_3}^{l_1 l_2 l_3}$ is a Clebsch-Gordan coefficient, and σ_l and δ_l are Coulomb and distorted-wave phase shifts, respectively. We note here that Eq. (5) corrects a typographical error in the denominator of Eq. (9) of [24]. The function $P_{l_1 l_2}^{LS}(k_1, k_2, T)$ is formed by projecting the final two-electron radial wave function (after propagation to a sufficiently long time T) $P_{l_1 l_2}^{LS}(r_1, r_2, t = T)$ onto the one-electron continuum orbitals.

Our two-electron TDCC calculations used a radial mesh of $(960)^2$ points with variable mesh spacing of between 0.01 and 0.2 a.u. [24]. We found that it was necessary to include partial-wave contributions from $L = 0$ to 14 to completely converge our calculations. We also note that, for all partial waves except $L = 0$, we include both "odd" and "even" parity contributions for each partial wave L. These contributions are the result of the increased coupling possibilities afforded by an initial p orbital, and such contributions have been included in previous TDCC calculations from initial p states, such as [26]. As an example, when considering the $L = 1$ partial wave, the natural parity channels that contribute to the $l_1 l_2$ expansion in Eq. (1) are ps, sp, pd, dp, df, fd, etc. However, the initial p orbital can also couple to the p channel of the wave packet to result in an overall symmetry of $L = 1$, with coupled channels pp, dd, ff, etc. This state has even parity. Such "opposite" parity states are usually termed "unnatural" parity contributions in previous work, for example, [27]. Studies of unnatural parity states have been conducted in positron scattering systems [28] and in cold atomic gases [29].
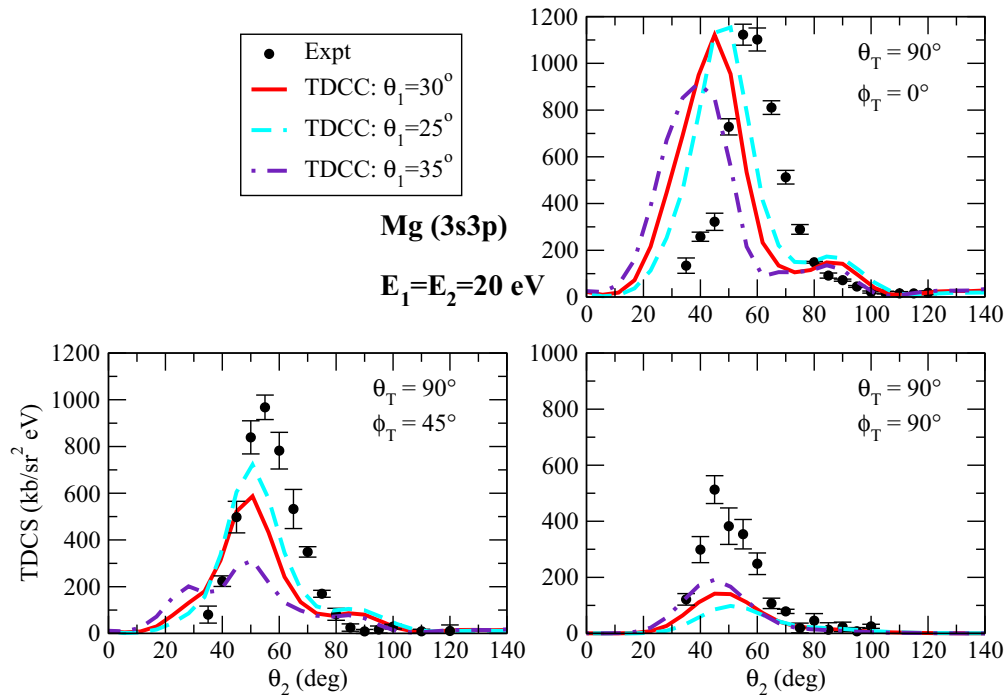
FIG. 2. (Color online) Triple differential cross sections for the electron-impact ionization of excited-state Mg for equal energy sharing between the outgoing electrons of $E_1 = E_2 = 20$ eV. The measurements of [17] are compared with TDCC calculations for various (θ_T,ϕ_T) orientations of the target $3p$ orbital as indicated. We present TDCC calculations performed at a fixed θ_1 angle of $30°$ (the fixed angle reported in the measurements of [17]) (solid red lines) and at angles of $25°$ (dashed blue lines) and $35°$ (dot-dashed purple lines).

III. RESULTS

We first compare our two-electron TDCC calculations to the measurements of Nixon and Murray [17] in Fig. 2. We show the triple differential cross section for three orientations of the aligned $3p$ orbital with respect to the scattering plane, for equal energy sharing between the outgoing electrons. The aligned p state is shown in the perpendicular geometry $(\theta_T = 90°, \phi_T = 90°)$ in Fig. 1. Since the measurements have an uncertainty of $\pm 5°$ in the scattered and ejected electron angular measurements, we show calculations for a fixed angle both of $30°$ (as reported in [17]) and of 25 and $35°$. We find for $\theta_T = 90°, \phi_T = 0°$ [i.e., the x-axis geometry] that the TDCC calculations are in quite good agreement with the measurement, with the TDCC calculations at the smaller fixed angle in slightly better agreement. For the geometry where the $3p$ orbital is along the y axis as in Fig. 1, we find that the TDCC calculations are in good agreement with experiment as to the position of the peak in the triple differential cross section, but are lower in magnitude than the measured values. We note that the relative measurements are normalized to the TDCC calculations for the largest cross section value in the $\theta_T = 90°, \phi_T = 0°$ case, and that this normalization then fixes the relative measurements at other orientations.

We note that the TDCC calculations in the y-axis case $(\theta_T = 90°, \phi_T = 90°)$ are clearly not zero, which differs from the identically zero 3DW calculations in this plane that were recently reported [20]. The TDCC cross sections are, however, significantly lower than the measured values. We have investigated the TDCC calculations at this geometry, and find that the usually dominant natural parity contributions

to each partial wave (i.e., the coupling of the two outgoing electrons into $^{1,3}S^e$, $^{1,3}P^o$, $^{1,3}D^e$, etc.) do in fact produce zero contribution to the cross section because the $M = +1$ and -1 contributions cancel exactly, as found in the distorted-wave calculations reported in [20]. In this geometry the $M = 0$ contribution is also identically zero. However, the unnatural parity contributions (i.e., $^{1,3}P^e$, $^{1,3}D^o$, etc.) are such that the $M = +1$ and -1 contributions do *not* cancel, but instead add (equally), producing a nonzero total cross section in this plane. The noncancellation for the opposite parity contributions can be traced to a phase factor, $(-1)^{l_1+l_2+L}$, that arises in the Clebsch-Gordan coefficient in the last term in Eq. (6). This phase factor produces an extra component of (-1) when comparing the $M = +1$ and -1 terms, which cancels the additional (-1) factor arising from the spherical harmonic terms for $Y_{lM=+1}$ and $Y_{lM=-1}$ (this latter factor was discussed in detail by Amami *et al.* [20]). For the natural parity terms, the $(-1)^{l_1+l_2+L}$ factor always results in $+1$, so that an overall cancellation of the $M = +1$ and -1 terms occurs. The 3DW calculations of Amami *et al.* [20] do not contain the unnatural parity contributions and therefore predict an identically zero cross section in this geometry.

Therefore, we find that the measured cross section in the y-axis geometry *directly* probes the unnatural parity contributions to the triple differential cross sections from ionization of excited-state Mg. Such contributions only occur for non-s state atomic targets. We are unaware of any previous ionization measurements that have probed such states. To further explore the effect of the unnatural parity contributions, in Fig. 3 we show TDCC calculations for a fixed angle of $30°$ (as in Fig. 2) and also TDCC calculations where the unnatural parity
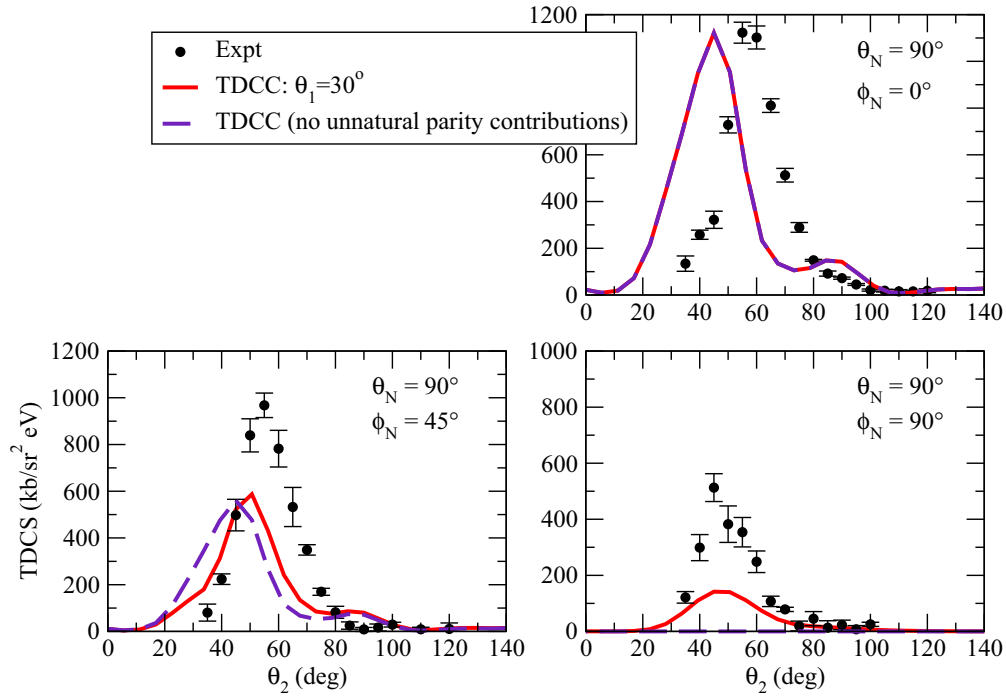
FIG. 3. (Color online) Same as Fig. 2, except now we show only the $\theta_1 = 30°$ TDCC calculation. We also present a TDCC calculation (purple dashed lines) in which the unnatural parity contribution is omitted.

contributions have been omitted. We find that the unnatural parity terms make no contribution for the x-axis geometry, which is also a consequence of the phase factors that enter the

Clebsch-Gordan coefficients in Eq. (6). For the case where the alignment is at $45°$ between the x and y axes, we find that the unnatural parity contribution is small, but noticeable,
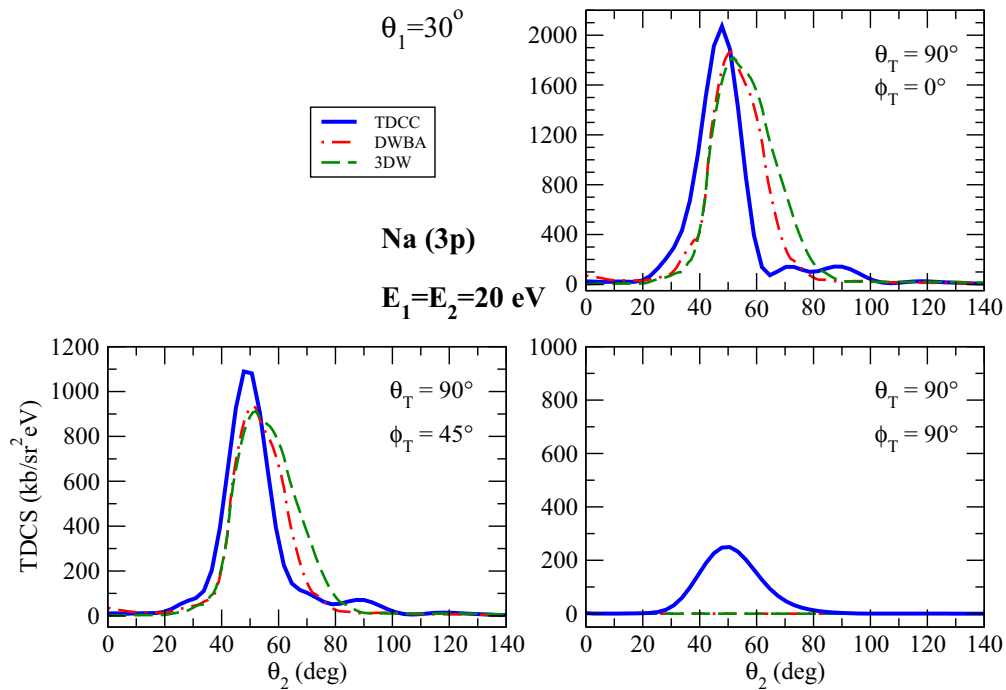

FIG. 4. (Color online) Triple differential cross sections for the electron-impact ionization of excited-state Na for equal energy sharing between the outgoing electrons of $E_1 = E_2 = 20$ eV. The cross sections are presented for a fixed electron angle of $\theta_1 = 30°$ and at various orientations of the $3p$ orbital as indicated. We compare the TDCC calculations (solid blue lines) with DWBA (dot-dashed red lines) and 3DW calculations (dashed green lines) made in a similar manner to the distorted-wave calculations presented in [20]. In this figure, the DWBA and 3DW calculations have been normalized to the TDCC calculations.

and inclusion of these terms moves the TDCC calculations towards the measured cross sections. We also note that omitting the unnatural parity contribution in this case results in a cross section that is exactly one half of the cross section computed for the x-axis geometry. This property was noted for the 3DW calculations presented in [20], and we find that this only holds in the TDCC calculations when the unnatural parity terms are omitted.

It is of interest to explore whether or not the nonzero cross section in the perpendicular geometry is also found for other systems. In Fig. 4 we present the electron-impact ionization of excited-state Na for the same alignment angles as in Fig. 2. Although no measurements are available for excited-state Na, we find that the cross sections from TDCC calculations for Na appear quite similar to those for Mg, and that the y-axis cross section is again nonzero. The TDCC calculation for ionization of the quasi-one-electron Na(3p) target may be considered more "robust" than the corresponding calculation for Mg, since the use of a two-active-electron approximation in the TDCC calculations for ionization of Na(3p) is well justified. In Fig. 4 we also compare with new distorted-wave Born approximation (DWBA) and 3DW calculations that were made in a similar manner to those recently made for Mg [20]. The TDCC and distorted-wave calculations are in reasonable agreement for the x-axis geometry ($\theta_T = 90°$, $\phi_T = 0°$) and the xy geometry ($\theta_T = 90°$, $\phi_T = 45°$), and we again find that the 3DW calculations predict an identically zero cross section for the y-geometry case ($\theta_T = 90°$, $\phi_T = 90°$).

As a further confirmation of the nonzero cross section in the perpendicular geometry from excited p-state atoms, we have also performed new calculations and measurements of the angular distributions of excited-state Ca in its 4s4p state. The TDCC calculations for Ca required finer radial meshes and inclusion of angular momentum states up to $L = 16$ to converge the calculations. New experiments were also performed on Ca using a similar apparatus to the measurements made on excited-state Mg [17,18]. In Fig. 5 we present the TDCS for Ca (4s4p) at equal energy sharing between the electrons of 30 eV. The upper panel shows the x-axis geometry cross sections and the lower panel shows the perpendicular geometry (y-axis) cross sections. Because our calculations indicate that the cross section is quite sensitive to the fixed-angle value, we present TDCC calculations averaged over the experimental angular uncertainties, as well as the individual TDCC calculations at each fixed angle. The measurements again find a nonzero cross section in the perpendicular geometry. The TDCC Ca calculations also find a nonzero cross section, although the position of the peak of the cross section is at slightly higher angles compared to the measurement. For the scattering plane cross sections shown in the upper panel, the TDCC calculations at a fixed angle of 45° find a peak that is at significantly lower angles than the measured cross section peak. However, calculations at lower values of the fixed angle appear to move closer to the measured values and also show that the cross section exhibits a strong sensitivity to the fixed-angle value. We note that a calculation at a fixed-angle value of 35° (not shown) is reasonably close to the measured cross section, but this is outside the measurement uncertainty of ±5° in the fixed-angle value. Figure 5 also shows 3DW calculations made for Ca in a similar manner to those made for Na and Mg. The 3DW
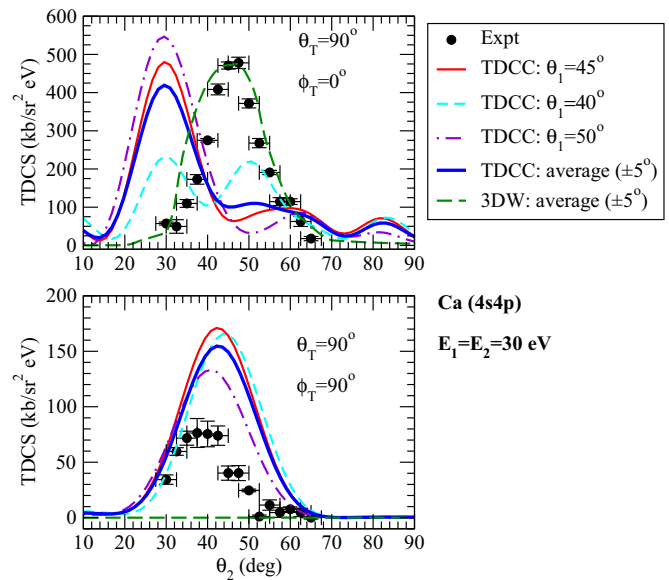

FIG. 5. (Color online) Triple differential cross sections for the electron-impact ionization of excited-state Ca for equal energy sharing between the outgoing electrons of $E_1 = E_2 = 30$ eV. Measurements are compared with TDCC calculations (solid blue lines) and 3DW calculations (green dashed line) as described in the text. The measurements were made for a fixed electron angle of 45°. The upper panel shows the cross section for the 4p orbital in the scattering plane and the lower panel shows the cross section for the 4p orbital perpendicular to the scattering plane. The thick solid blue lines indicate a TDCC calculation averaged over the experimental angular uncertainties, while the thin (solid red, dashed light blue, dot-dashed purple) lines show the individual TDCC calculations at each fixed angle.

calculations are in good agreement with the measurement for the x-axis case in the upper panel but again predict a zero cross section for the y-axis case. DWBA calculations (not shown) are very similar to the 3DW calculations presented here.

Finally, we note that a three-electron TDCC method can also be applied to the computation of the single ionization of Mg or Ca, in a similar manner to the calculations used for the electron-impact double ionization of Mg that were recently reported [30]. Such three-electron calculations have an advantage compared to two-electron calculations in that one can construct the initial state to be the $3s3p$ ^1P term, which of course is the real initial state of the measurements with which we compare here. However, such three-electron calculations are significantly more computationally intensive than the two-electron calculations reported in this manuscript. Complete convergence of the three-electron calculations in terms of all the angular momenta up to $L = 14$ and using a sufficiently large radial mesh is not yet possible given current computational resources. We do find that preliminary calculations using just a few partial waves of our three-electron TDCC approach indicate that the TDCS in the perpendicular geometry is again not zero and has a peak in the cross section at similar angles to the cross sections presented in Fig. 2. This indicates that our configuration-average approach for

the ionization of Mg $3s3p$ and Ca $4s4p$ may not be too severe an approximation. In future work we plan to continue our three-electron TDCC investigations and hope that a fully converged calculation is feasible sometime soon.

IV. CONCLUSION

In summary, we have presented evidence using TDCC calculations that the measured cross section from ionization of excited-state laser-aligned atoms that are perpendicular to the scattering plane arise solely from unnatural parity contributions to the ionization amplitude. Although the overall agreement between the TDCC calculations and the measured cross sections is only moderately good, our calculations help resolve the discrepancy with the zero cross section predicted by distorted-wave approaches for ionization in this geometry.

[1] E. Weigold and I. E. McCarthy, *Electron Momentum Spectroscopy* (Plenum, New York, 1999).

[2] T. N. Rescigno, M. Baertschy, W. A. Isaacs, and C. W. McCurdy, Science **286**, 2474 (1999).

[3] M. Baertschy, T. N. Rescigno, W. A. Isaacs, X. Li, and C. W. McCurdy, Phys. Rev. A **63**, 022712 (2001).

[4] I. Bray, J. Phys. B **33**, 581 (2000).

[5] I. Bray, Phys. Rev. Lett. **89**, 273201 (2002).

[6] I. Bray, K. Bartschat, and A. T. Stelbovics, Phys. Rev. A **67**, 060704 (2003).

[7] J. Colgan and M. S. Pindzola, Phys. Rev. A **74**, 012713 (2006).

[8] I. Bray, D. V. Fursa, J. Röder, and H. Erhardt, J. Phys. B **30**, L101 (1997).

[9] S. Rioual, J. Röder, B. Rouvellou, H. Erhardt, A. Pochat, I. Bray, and D. V. Fursa, J. Phys. B **31**, 3117 (1998).

[10] A. T. Stelbovics, I. Bray, D. V. Fursa, and K. Bartschat, Phys. Rev. A **71**, 052716 (2005).

[11] J. Colgan, M. S. Pindzola, G. Childers, and M. A. Khakoo, Phys. Rev. A **73**, 042710 (2006).

[12] M. Dürr, C. Dimopoulou, B. Najjari, A. Dorn, and J. Ullrich, Phys. Rev. Lett. **96**, 243202 (2006).

[13] M. Dürr, C. Dimopoulou, A. Dorn, B. Najjari, I. Bray, D. V. Fursa, Z. Chen, D. H. Madison, K. Bartschat, and J. Ullrich, J. Phys. B **39**, 4097 (2006).

[14] O. Al-Hagan, C. Kaiser, D. H. Madison, and A. J. Murray, Nature Physics **5**, 59 (2008).

[15] J. Colgan, M. S. Pindzola, F. Robicheaux, C. Kaiser, A. J. Murray, and D. H. Madison, Phys. Rev. Lett. **101**, 233201 (2008).

[16] J. Colgan, O. Al-Hagan, D. H. Madison, C. Kaiser, A. J. Murray, and M. S. Pindzola, Phys. Rev. A **79**, 052704 (2009).

[17] K. L. Nixon and A. J. Murray, Phys. Rev. Lett. **106**, 123201 (2011).

[18] K. L. Nixon and A. J. Murray, Phys. Rev. Lett. **112**, 023202 (2014).

[19] X. Ren, T. Pflüger, S. Xu, J. Colgan, M. S. Pindzola, A. Senftleben, J. Ullrich, and A. Dorn, Phys. Rev. Lett. **109**, 123202 (2012).

[20] S. Amami, A. Murray, A. Stauffer, K. L. Nixon, G. S. J. Armstrong, J. Colgan, and D. H. Madison, Phys. Rev. A **90**, 062707 (2014); **91**, 069906(E) (2015).

[21] A. D. Stauffer, Phys. Rev. A **89**, 032710 (2014); **89**, 049906(E) (2014).

[22] M. S. Pindzola, F. Robicheaux, S. D. Loch, J. C. Berengut, T. Topcu, J. Colgan, M. Foster, D. C. Griffin, C. P. Ballance, D. R. Schultz, T. Minami, N. R. Badnell, M. C. Witthoeft, D. R. Plante, D. M. Mitnik, J. A. Ludlow, and U. Kleiman, J. Phys. B **40**, R39 (2007).

[23] J. Colgan and M. S. Pindzola, Euro. Phys. J. D **66**, 11 (2012).

[24] G. S. J. Armstrong, J. Colgan, and M. S. Pindzola, Phys. Rev. A **88**, 042713 (2013).

[25] M. E. Rose, *Elementary Theory of Angular Momentum* (Wiley, New York, 1967).

[26] J. Colgan, M. S. Pindzola, D. M. Mitnik, D. C. Griffin, and I. Bray, Phys. Rev. Lett. **87**, 213201 (2001).

[27] J. Eiglsperger, B. Piraux, and J. Madroñero, Phys. Rev. A **81**, 042528 (2010).

[28] M. Umair and S. Jonsell, J. Phys. B **47**, 225001 (2014).

[29] D. Rakshit, K. M. Daily, and D. Blume, Phys. Rev. A **85**, 033634 (2012).

[30] M. S. Pindzola, J. A. Ludlow, F. Robicheaux, J. Colgan, and D. C. Griffin, J. Phys. B **42**, 215204 (2009).